

RESEARCH ARTICLE

Open Access



Further structure–activity relationships study of substituted dithiolethiones as glutathione-inducing neuroprotective agents

Dennis A. Brown^{1*} , Swati Betharia¹, Jui-Hung Yen², Ping-Chang Kuo² and Hitesh Mistry¹

Abstract

Background: Parkinson's disease is a neurodegenerative disorder associated with oxidative stress and glutathione depletion. The induction of cellular glutathione levels by exogenous molecules is a promising neuroprotective approach to limit the oxidative damage that characterizes Parkinson's disease pathophysiology. Dithiolethiones, a class of sulfur-containing heterocyclic molecules, are known to increase cellular levels of glutathione; however, limited information is available regarding the influence of dithiolethione structure on activity. Herein, we report the design, synthesis, and pharmacological evaluation of a further series of dithiolethiones in the SH-SY5Y neuroblastoma cell line.

Results: Our structure–activity relationships data show that dithiolethione electronic properties, given as Hammett σ_p constants, influence glutathione induction activity and compound toxicity. The most active glutathione inducer identified, **6a**, dose-dependently protected cells from 6-hydroxydopamine toxicity. Furthermore, the protective effects of **6a** were abrogated by the inhibitor of glutathione synthesis, buthionine sulfoximine, confirming the importance of glutathione in the protective activities of **6a**.

Conclusions: The results of this study further delineate the relationship between dithiolethione chemical structure and glutathione induction. The neuroprotective properties of analog **6a** suggest a role for dithiolethiones as potential antiparkinsonian agents.

Keywords: Neuroprotection, Parkinson's disease, Glutathione, Dithiolethiones

Background

The incidences of neurodegenerative disorders are expected to greatly increase as the American population ages. Parkinson's disease (PD), the second most common neurodegenerative disease, is a movement disorder characterized by the gradual disintegration of the nigrostriatal dopaminergic pathway. The resulting depletions of striatal dopamine (DA) give rise to the cardinal symptoms of the disease, including tremor, rigidity, bradykinesia, and postural instability. Additionally, cognitive issues, depression, and sleep disturbances are frequently observed non-motor symptoms. Although pharmacotherapeutic

intervention is capable of providing symptomatic relief in PD, to date no therapy is able to arrest or reverse the progression of the disease.

The cause of PD is not currently fully understood; however, the etiology of sporadic PD, the most prevalent form of the disease, is probably multifactorial, involving a combination of genetic, environmental, and unknown factors. Increasingly, oxidative stress is emerging as a major player in neurodegenerative disorders such as PD. Analyses of the brains of PD patients have demonstrated extensive cellular damage caused by oxidative stress [1]. Neurons may be particularly prone to oxidative damage due to their high lipid content and oxygen consumption. Dopaminergic neurons experience an additional oxidative burden due to the autoxidation and metabolism of DA. These processes yield damaging

*Correspondence: dabrown@manchester.edu

¹ Department of Pharmaceutical Sciences, Manchester University College of Pharmacy, 10627 Diebold Rd, Fort Wayne, IN 46845, USA
Full list of author information is available at the end of the article

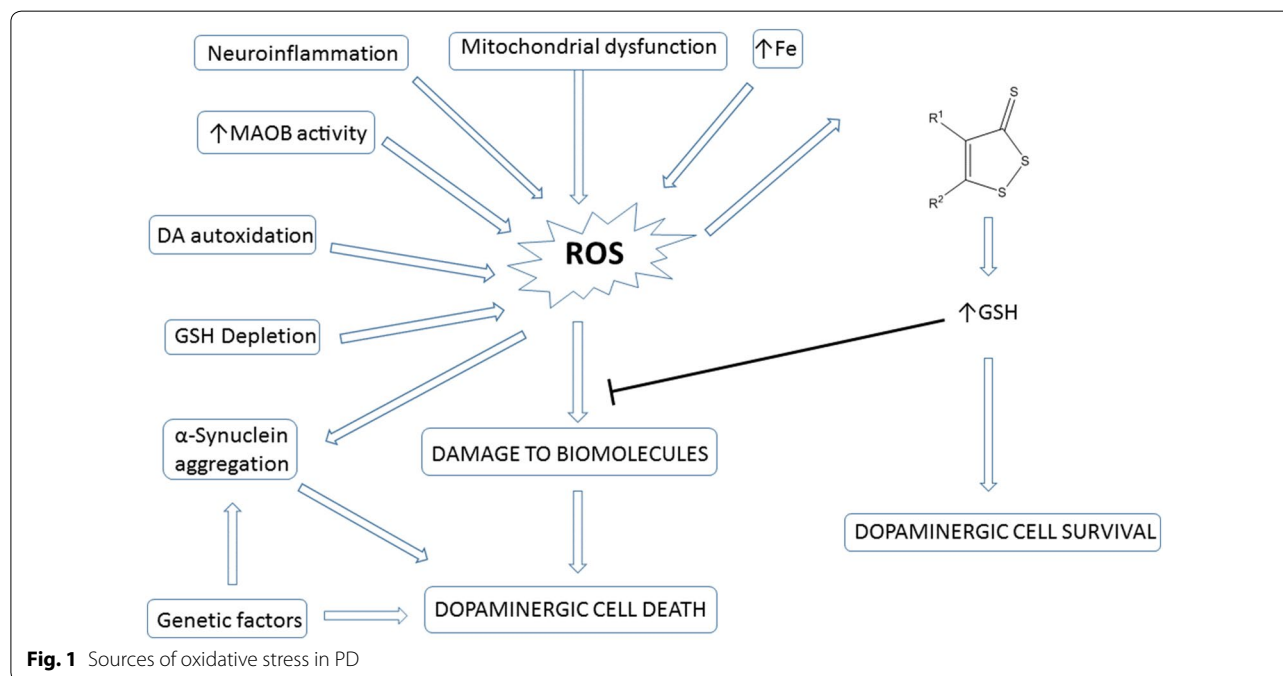
electrophilic DA-quinones and reactive oxygen species (ROS). Additionally, many of the molecular hallmarks of PD, such as mitochondrial dysfunction, α -synuclein aggregation, neuroinflammation, increased monoamine oxidase B activity, and elevated levels of iron, are related to increased oxidative activity [2–7]. ROS cause lipid peroxidation, protein and DNA damage, and ultimately the demise of dopaminergic neurons [8–10] (Fig. 1).

As reactive oxygen species occur naturally in all cells, various antioxidants and enzymes have been evolved to mitigate their harmful effects. Glutathione (GSH), a cysteine-containing tripeptide, is the most abundant non-protein antioxidant in the body, and plays a crucial role in the detoxification of ROS and dopamine metabolites [11]. GSH can detoxify ROS non-enzymatically, forming oxidized glutathione (GSSG). GSH also serves as a cosubstrate for several phase II enzymes. Glutathione *S*-transferase (GST) mediates the addition of GSH to electrophiles, such as dopamine *o*-quinone, and glutathione peroxidase (GPx) catalyzes the reduction of peroxides, including H_2O_2 [12, 13]. However, in PD, the oxidative load experienced by dopaminergic neurons overwhelms these endogenous cellular detoxification mechanisms. Indeed, postmortem analyses of the brains of PD patients have shown depleted levels of nigrostriatal GSH [14]. As such, increasing neuronal levels of GSH may provide therapeutic benefit against the damaging effects of oxidative stress in PD.

The rate-limiting step in the biosynthesis of GSH is mediated by glutamate cysteine ligase (GCL). Associated

with the gene of this enzyme is the antioxidant response element (ARE), found in many genes that play a role in protecting cells from oxidative damage, including GCLC (the catalytic subunit of GCL), GST, GPx, NAD(P)H:quinone oxidoreductase (NQO1), superoxide dismutase, hemeoxygenase, catalase, and many others [15]. Stabilization and nuclear translocation of the transcription factor Nrf2 (nuclear factor-erythroid-2 related factor-2) enhances the transcription of ARE-associated genes [16]. Nrf2 is a short-lived protein, undergoing rapid ubiquitination and proteasomal degradation under basal conditions, mediated by its repressor Keap1 (Kelch-like ECH-associated protein-1) [17–19]. Keap1 is a cysteine-rich protein that serves as a sensor of oxidative and electrophilic stress. The stabilization of Nrf2 is believed to involve modulation of some of the numerous cysteine residues of Keap1 by ROS and electrophiles, leading to enhanced Nrf2 stability and nuclear accumulation [20–22].

Dithiolethiones (DTTs) are a class of sulfur-containing heterocycles (Fig. 2). DTTs have been shown to induce the expression of a variety of ARE-associated detoxification enzymes and molecules, including GCLC and GSH, in numerous cell and tissue types; however, limited information is available regarding the activities of these interesting molecules in the CNS [23–25]. Our group is interested in exploring GSH induction as a potential neuroprotective strategy. In a previous report by our group, we described a preliminary SAR study of substituted DTTs as inducers of GSH in the SH-SY5Y neuroblastoma



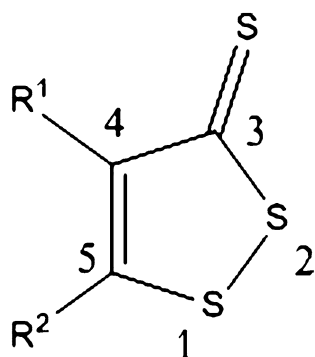


Fig. 2 Generalized structure of dithiolethiones

cell line (a dopaminergic cell line commonly employed in *in vitro* models of PD), with key findings that placement of electron withdrawing groups (EWGs) at the 4-position and electron donating groups (EDGs) at the 5-position induced the most glutathione [26–28]. Additionally, three of these GSH inducers demonstrated neuroprotection in the *in vitro* 6-hydroxydopamine (6-OHDA) model of neurotoxicity. Based on these initial findings, we sought to better understand the influence of DTT substituents on GSH induction. In this report, we describe the synthesis and GSH induction activities of additional substituted DTTs. The relationship between DTT structure and pharmacological activity is discussed.

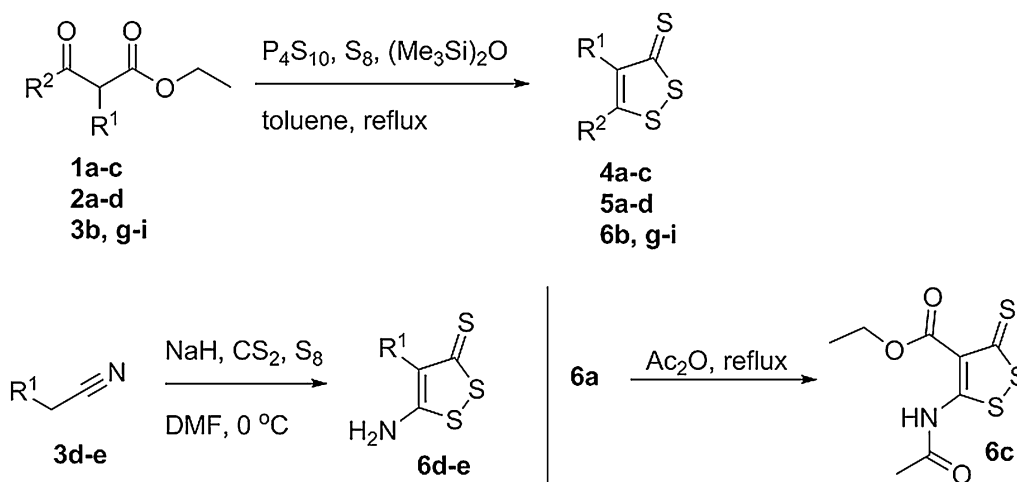
Chemistry

A series of 4-, 5-, and 4, 5-disubstituted DTTs was synthesized (Table 1) to determine the generality of the initial SAR findings previously communicated by us [26]. These molecules were designed to ensure that a diversity of electronic features were represented in the

Table 1 Structures and Hammett sigma constants of DTTs

Entry	R ¹ (σ_p) [31]	R ² (σ_p) [31]	Entry
–	H	H	D3T
1a	4-NO ₂ -C ₆ H ₄ (0.26)	H (0)	4a
1b	Ethyl (−0.15)	H (0)	4b
1c	CO ₂ Et (0.50)	H (0)	4c
2a	H (0)	Me (−0.17)	5a
2b	H (0)	4-F-C ₆ H ₄ (0.06)	5b
2c	H (0)	4-pyridinyl (0.44)	5c
2d	H (0)	2-furanyl (0.02)	5d
3a	CO ₂ Et (0.50)	NH ₂ (−0.66)	6a
3b	CO ₂ Et (0.50)	Me (−0.17)	6b
3c	CO ₂ Et (0.50)	NHC(O)Me (0.00)	6c
3e	4-Cl-C ₆ H ₄ (0.12)	NH ₂ (−0.66)	6d
3d	SO ₂ Ph (0.68)	NH ₂ (−0.66)	6e
3f	CN (0.66)	NH ₂ (−0.66)	6f
3g	Cl (0.23)	4-OMe-C ₆ H ₄ (−0.08)	6g
3h	Cl (0.23)	C ₆ H ₅ (−0.01)	6h
3i	Cl (0.23)	Ethyl (−0.15)	6i

compounds evaluated, including various aryl, alkyl, and amino groups, with both electron donating and electron withdrawing properties. The syntheses of DTTs are shown in Scheme 1. Compounds **4a–c**, **5a–d**, and **6b, g–i** were synthesized from requisite β -keto esters by treatment with P₄S₁₀, S₈, and (Me₃Si)₂O in refluxing toluene for 1–3 h in good to excellent yield [29]. Molecules **6d–e** were synthesized from their corresponding nitriles via reaction with NaH, S₈, and CS₂ in DMF at 0 °C for 30 min, in excellent yield [30]. Compound **6c** was synthesized by refluxing **6a** in acetic anhydride for 30 min (Scheme 1). Molecules **6a** and **6f** were purchased commercially.



Scheme 1 Synthesis of dithiolethiones

Results and discussion

DTTs were assayed for GSH induction. SH-SY5Y human neuroblastoma cells were treated with test compounds for 24 h at a concentration of 100 μ M. The results are shown in Fig. 3 and are reported as a percentage of control. Among the four 5-substituted DTTs (**5a–d**) evaluated, electron-donating 5-methyl substituted DTT **5a** induced GSH to the highest extent (163 %) compared to the other 5-substituted DTTs evaluated. Compounds **5b**, **5c**, and **5d**, each containing electron-withdrawing aromatic groups, induced a lesser amount of GSH (94, 114 and 130 %, respectively). These results are consistent with our previous findings that alkyl groups at this position are superior to aromatic groups.

Next evaluated were three 4-substituted molecules, **4a–c**, containing *p*-nitrophenyl, ethyl, and ester groups, respectively. Interestingly, electronically-different **4a** and **4b** increased GSH levels by almost the same extent (156 % for **4a**, and 149 % for **4b**). The activity of **4b** is unexpected, as our previous work suggested that EDGs at this position would induce less GSH as their electron-withdrawing counterparts. Surprisingly, when 4-ethyl ester substituted analog **4c** was tested, significant toxicity was observed, and the GSH induction data for this compound was omitted (*vide infra*).

Next, we explored the effects on GSH induction of substituting both the 4- and 5-positions of the DTT core with a variety of functional groups (compounds **6a–i**). The most active molecule in this series was analog **6a** (4-ethyl ester, 5-amino), which increased cellular GSH levels by 190 %. Interestingly, replacement of the primary amine of **6a** with a methyl group, **6b**, significantly reduced activity. Similarly, substitution of the ester of **6a** with an aryl ring (**6d**) or chloro group (**6g–i**), diminished

activity, regardless of the nature of the 5-position. The SAR data from disubstituted DTTs suggest that GSH induction is highest when the 4- and 5-positions possess strongly electron withdrawing and strongly electron donating groups, respectively. Compounds **6e** (4-phenyl-sulfonyl, 5-amino) and **6f** (4-nitrile, 5-amino) exhibited toxicity when evaluated and the resulting GSH induction data were omitted (*vide infra*).

The above SAR data demonstrate that electronic parameters influence GSH induction activity. As such, we sought a method to quantitatively assess the electronic properties of substituted DTTs. We decided to explore Hammett's σ_p constants (Table 1), which reflect the ability of substituted benzoic acids to stabilize a negatively charged carboxylate upon ionization of the corresponding acid. The constants given for these ionizations are an indication of the release ($-\sigma_p$) or withdrawal ($+\sigma_p$) of electrons by a substituent, and provide an indication of the combined contributions of both inductive and resonance effects. We plotted our GSH induction values for 4- and 5-substituted compounds from this and our previous study (structures shown in Table 2) against reported Hammett σ_p constants (Fig. 4) [31]. As EDGs at the 5-position were observed to be beneficial to activity, we chose to use $+\sigma_p$ for these types of functional groups, and $-\sigma_p$ for EWGs, which appeared to impair GSH induction. Analogously, as EWGs generally had a positive influence on activity at the 4-position, we used $+\sigma_p$; $-\sigma_p$ were employed for the less active EDGs. As can be seen in Fig. 4a, a linear relationship was observed between DTT electronic properties and GSH induction, with only two molecules, **4b** and **5c**, laying outside of the curve ($r^2 = 0.7969$ with **4b** and **5c** omitted). Interested in whether electronics similarly influence activity for the 4,

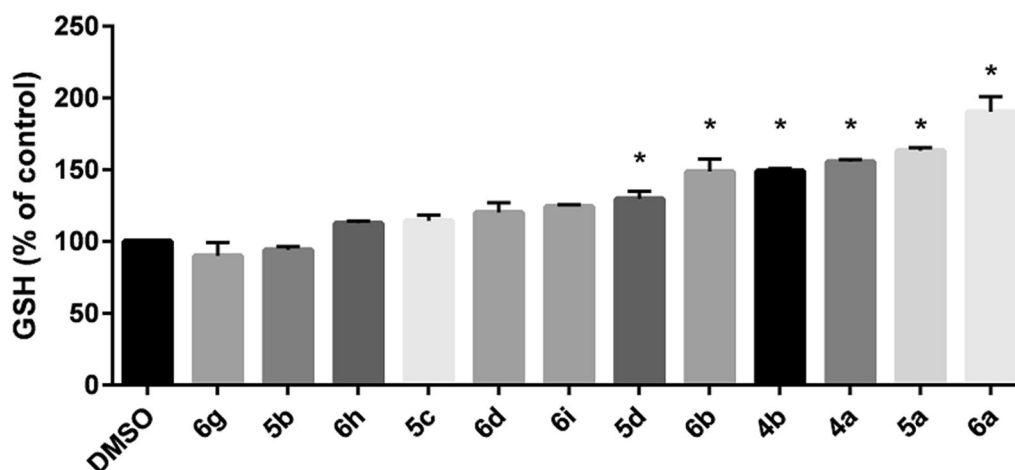


Fig. 3 DTT-mediated GSH induction. SH-SY5Y cells were treated with test compounds (100 μ M) for 24 h, at which time total cellular GSH was measured. Data shown are mean \pm SEM of at least three different experiments. * $P < 0.05$

Table 2 DTT structures from initial SAR study and corresponding Hammett sigma constants [26, 31]

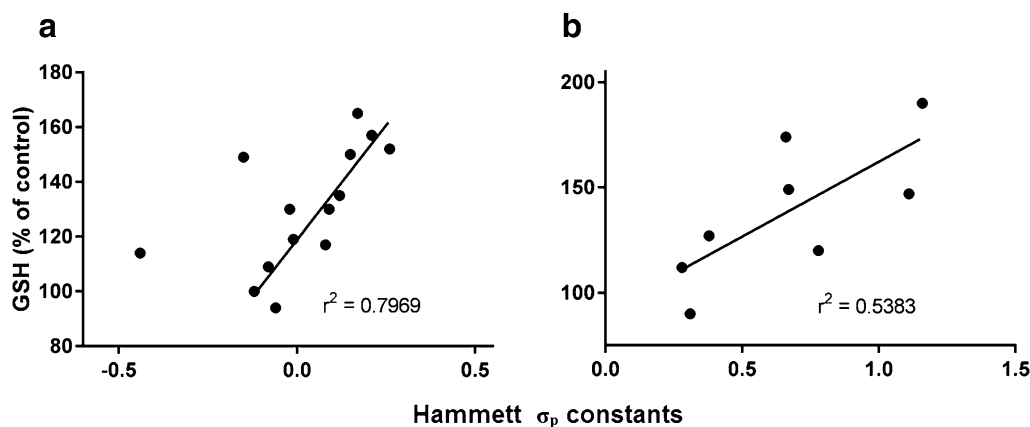
R ¹ (σ_p)	R ² (σ_p)	Entry
4-OMe-C ₆ H ₄ (−0.08)	H (0)	4d
C ₆ H ₅ (−0.01)	H (0)	4e
CH ₂ CF ₃ (0.09)	H (0)	4f
4-Cl-C ₆ H ₄ (0.12)	H (0)	4g
H (0)	Ethyl (−0.15)	5e
H (0)	Cyclopropyl (−0.21)	5f
H (0)	4-Cl-C ₆ H ₄ (0.12)	5g
H (0)	4-OMe-C ₆ H ₄ (−0.08)	ADT

5-disubstituted molecules, we summed the σ_p constants of both substituents (using the same approach to the sign of σ_p described above) and plotted these values with the respective GSH activity. Again, a relationship was seen, supporting the influence of electronic properties on GSH induction ($r^2 = 0.5383$, Fig. 4b).

As previously mentioned, when DTTs **4c**, **6e**, and **6f** were evaluated for GSH induction in SH-SY5Y cells, significant toxicity was observed, and the GSH induction data for these molecules was omitted from the study. Interestingly, analogs **6a** and **6b**, amino and methyl 5-substituted congeners of **4c**, appeared to not be toxic to SH-SY5Y cells. Based on this observation, we began to suspect that DTT toxicity may be related to the value of σ_p at the 4-position. To test this hypothesis, we measured the viability of SH-SY5Y cells treated with our DTTs (100 μ M, 24 h, Fig. 5). Molecules with 4-position σ_p constants ranging from −0.15 (**4b**) to 0.26 (**4a**) showed minimal toxicity to SH-SY5Y cells. However, when the σ_p constant was raised to 0.50 (**4c**), significant cell death was seen. Surprisingly, the addition of an amino or methyl substituent to the 5-position of **4c** (compounds **6a** and

6b, respectively) appeared to restore viability. To confirm the beneficial effects on toxicity of an electron-donating group at the 5-position, the amino group of **6a** was acylated, yielding **6c**. As the σ_p constant of the acetamide group is 0.0, electron donation should not take place, and **6c** would be expected to be toxic. This was indeed observed as shown by the restoration of toxicity of **6c**. The beneficial effects of placing electron-donating substituents at the 5-position appears to be limited, however. When the σ_p constant of the 4-position of **6a** (ethyl ester, $\sigma_p = 0.50$) was increased to 0.66 (nitrile, compound **6f**), or 0.68 (sulfone, compound **6e**), cell viability was once again decreased.

The above observation that GSH induction is dependent on the magnitude of Hammett σ_p constants suggests that DTTs substituents influence the reactivity of the dithiolethione ring. Stabilization of Nrf2 by DTTs is believed to result from alteration of the interaction between Nrf2 and its repressor, Keap1. In the presence of oxygen and cellular thiols, the DTTs D3T, oltipraz, and ADT generate superoxide anion, O₂^{•−}, a progenitor to H₂O₂ [32–34]. Either of these reactive oxygen species could oxidize the numerous sulfhydryl groups of Keap1, resulting in diminished ubiquitination and increased nuclear accumulation of Nrf2. The placement of substituents with larger σ_p constants on the dithiolethione ring may render the molecule more reactive to thiols, resulting in greater GSH induction. It is also likely that the toxicity observed by several of the evaluated DTTs may be a consequence of the above described mechanism of action. The DTTs that were observed to be toxic to SH-SY5Y cells (**4c**, **6c**, **6e** and **6f**) would be expected to induce more GSH than other evaluated DTTs, based on extrapolation of our GSH induction vs. σ_p plots. Given the current evidence for the proposed mechanism of action of Nrf2 activation by DTTs, it is possible that

**Fig. 4** GSH induction values of 4- and 5-substituted DTTs (**a**), and 4, 5-disubstituted DTTs (**b**) vs. Hammett σ_p constants

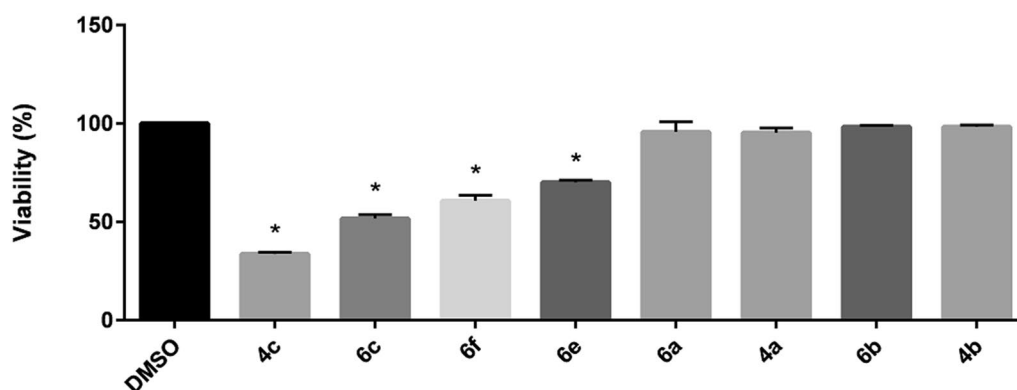


Fig. 5 Toxicity of DTTs. SH-SY5Y cells were treated with the indicated molecules (100 μ M) for 24 h, at which time viability was assessed. Data shown are mean \pm SEM of at least three different experiments. * $P < 0.05$

toxicity results from an increased level of reactive oxygen species produced from DTTs with higher σ_p constants for the 4-position. Additional studies are currently planned to more clearly understand the nature of DTT toxicity.

The observed influence of DTT substituent σ_p constants on GSH induction and compound toxicity has important implications in the design and selection of future molecules as neuroprotective agents. 4-Monosubstituted congeners must possess substituents with σ_p constants that are less than 0.5 to avoid toxicity, thus limiting the extent of GSH induction possible. Their 5-monosubstituted counterparts must have strongly electron-donating groups to effect significant GSH induction; however, aliphatic groups, the most active function group at this position, were only able to increase GSH by a maximum of 165 % (compound **5a**). Substitution of carbon-containing substituents at the 5-position with heteroatoms (O, N) would increase the electron donating effects at this site; however, efforts to synthesize such monosubstituted analogs proved to be problematic. Disubstituted DTT **6a** appears to solve both of these issues: the strongly electron withdrawing ester at the 4-position, combined with the electron donating 5-amino group, provide the large values of σ_p needed for maximal GSH induction. Additionally, the 5-amino group mitigates the toxicity that is associated a large σ_p value for the 4-position. As the values of DTT substituents cannot be increased much more without causing toxicity, it is likely that the activity of analog **6a** represents the upper limit of GSH induction for substituted DTTs.

Having identified a DTT that potentially increases cellular GSH levels, we next evaluated the ability of **6a** to protect against 6-OHDA induced toxicity, a commonly used neuroprotection model [35–38]. SH-SY5Y cells were pre-treated with **6a** for 24 h at concentrations of 6.25, 12.5, 25, 50, and 100 μ M, followed by concurrent exposure

to 40 μ M 6-OHDA for a further 24 h. Cell viability was then determined. As shown in Fig. 6 administration of 40 μ M 6-OHDA reduced cellular viability to 22 %. Excitingly, pretreatment with **6a** dose-dependently protected against the toxic effects of 6-OHDA. Protective effects were seen starting with a concentration of 12.5 μ M (33 % viability), and plateaued with the doses of 50 and 100 μ M; interestingly, these two doses were equally protective (56 and 58 %, respectively).

The mechanism of 6-OHDA toxicity involves the generation of ROS and electrophilic quinone metabolites [39]. The increase in cellular GSH levels mediated by **6a** likely protects against the oxidative insult of 6-OHDA. To explore the role that GSH plays in this protection, SH-SY5Y cells were co-treated with **6a** and buthionine

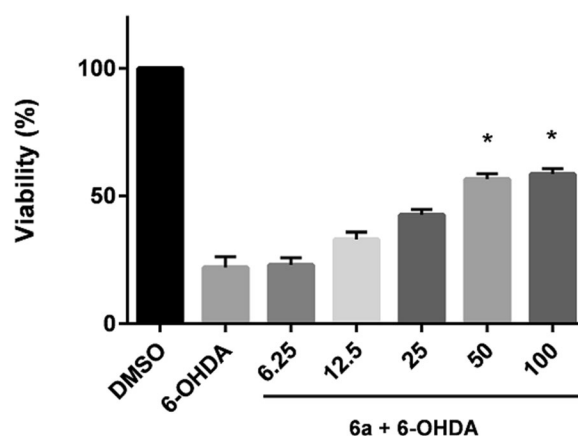


Fig. 6 Neuroprotection of **6a** against 6-OH induced neurotoxicity. SH-SY5Y cells were treated for 24 h with various concentrations of **6a**, followed by co-treatment with 6-OHDA (40 μ M) for a further 24 h, at which time cellular viability was assessed. Data shown are mean \pm SEM of at least three different experiments. * $P < 0.05$

sulfoximine (BSO), an inhibitor of GCLC [40]. As shown in Fig. 7, administration of BSO (25 μ M) was able to inhibit the ability of **6a** (100 μ M) to induce GSH, demonstrating that GSH induction is mediated through actions of GCLC. Additionally, the abrogation of GSH induction by BSO was able to block the neuroprotective effects of **6a** (Fig. 8), confirming the importance of GSH in neuroprotection. DTTs are known, via stabilization of Nrf2, to induce the expression of numerous cytoprotective phase II enzymes, and it is possible that the activity of these enzymes contribute to the protective effects of **6a**. However, as the protective effects of **6a** can be blocked by inhibition of GSH induction, the contribution to neuroprotection of other phase II enzymes in this model may be minimal.

Many of the symptoms of PD arise as a result of depletion of nigrostriatal DA levels. As such, current antiparkinsonian pharmacotherapeutic approaches are DA focused. These treatments aim to replace DA (levodopa), slow its metabolism (inhibitors of monoamine oxidase B and catecholamine O-methyltransferase), or supplement its effects (dopamine agonists). While these agents are able to provide symptomatic relief in PD, they do little to halt or reverse the progression of the disorder since they do not address the underlying oxidative damage that is responsible for the loss of dopaminergic neurons. The results of this study, while preliminary, suggest that elevation of cellular levels of GSH may have promise as a potential antioxidant-based antiparkinsonian approach. Additional studies are currently planned to examine the neuroprotective potential of DTTs in additional cell lines and PD models.

Conclusions

In support of our effort to identify novel potential neuroprotective agents, a further series of substituted DTTs was synthesized and evaluated for GSH induction in the

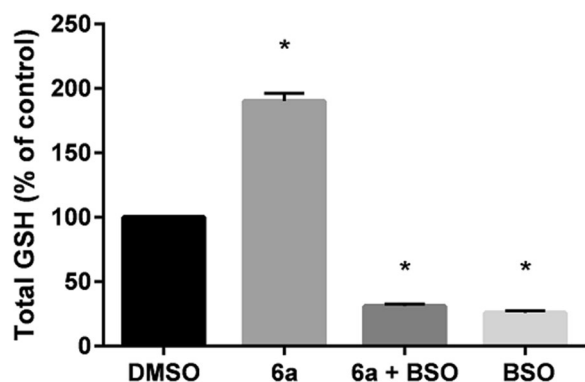


Fig. 7 Suppression of GSH induction of **6a** by BSO. SH-SY5Y cells were treated with **6a** (100 μ M) and/or BSO (25 μ M) for 24 h, at which time total cellular GSH levels were assessed. Data shown are mean \pm SEM of at least three different experiments. * $P < 0.05$

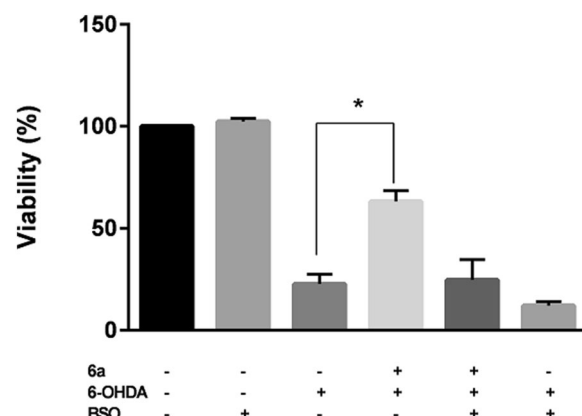


Fig. 8 Abrogation of protective neuroprotective effects of **6a** by BSO. SH-SY5Y cells were treated with **6a** (100 μ M) and/or BSO (25 μ M) for 24 h, at which time either 6-OHDA (40 μ M) or DMSO was added. Cellular viability was measured 24 h later. Data shown are mean \pm SEM of at least three different experiments. * $P < 0.05$

SH-SY5Y human neuroblastoma cell line. Our results showed that the extent of GSH induction is related to the electronic properties of DTTs. Plots of GSH induction vs. DTT substituent Hammett σ_p values demonstrated linear relationships for substituents of 4-, 5-, and 4, 5-disubstituted DTTs. It was also observed that the magnitude of σ_p at the 4-position influences DTT toxicity, which can be diminished by the presence of an EDG at the 5-position. The most potent inducer of GSH identified in this study, congener **6a**, was minimally toxic to cells and was able to provide neuroprotection in the 6-OHDA model of neurotoxicity, suggesting GSH induction as a neuroprotective strategy. GSH induction was shown to be crucial to neuroprotection, as the protective effects of **6a** were abrogated by treatment with the GCLC inhibitor, BSO. The data generated in this study suggest that dithiolethiones warrant additional exploration as potential neuroprotective, antiparkinsonian agents.

Experimental section

Chemistry methods

All solvents and reagents obtained from commercial sources were used without further purification, unless otherwise noted. Compounds **6a** and **6f** were purchased from Oakwood Chemical (West Columbia, SC) and purified prior to use. All reactions were carried out under an argon atmosphere unless otherwise noted. All final molecules were >95 % pure as judged by high-performance liquid chromatography (HPLC). HPLC analyses were performed on an Agilent 1220 Infinity system with an Agilent column (Poroshell 120 EC-C18, 4.6 \times 150 mm, gradient of 0.1 % trifluoroacetic acid/acetonitrile). ^1H and ^{13}C NMR analyses were performed on a Varian Mercury

300 MHz spectrophotometer at 300 and 75 MHz, respectively. Chemical shifts are given in ppm in reference to tetramethylsilane (TMS) as an internal standard. Multiplicities are given as s (singlet), d (doublet), t (triplet), m (multiplet), and br s (broad signal). Low-resolution mass spectral data were obtained on an Agilent 1260 Infinity single quadrupole LCMS system. Melting points were taken on a Mel-Temp apparatus and are uncorrected. Thin layer chromatography (TLC) was performed on silica gel 60 F₂₅₄-coated glass plates purchased from EMD Millipore, and visualized with UV light and/or basic KMnO₄.

General procedure for the synthesis of dithiolethiones from β -keto esters, exemplified by 5-methyl-3H-1,2-dithiole-3-thione, 5a [41]

To a suspension of elemental sulfur (123 mg, 3.85 mmol), phosphorus pentoxide (1.03 g, 2.31 mmol), hexamethyldisiloxane (2.76 mL, 11.6 mmol), in toluene (10 mL) was added β -oxo ester **2a** (500 mg, 3.85 mmol). The mixture was heated under reflux conditions until complete as judged by TLC (generally between 1 and 3 h), at which time the reaction mixture was cooled to 0 °C. Saturated aqueous K₂CO₃ was added (5 mL) to destroy any unreacted phosphorus pentoxide. The crude product was then extracted with ethyl acetate (10 mL \times 3), dried (Na₂SO₄), filtered, concentrated, and purified by column chromatography (hexanes/ethyl acetate, 4:1) to give a low-melting red solid (521 mg, 91 %). R_f = 0.65 (20 % EtOAc/Hex). ¹H NMR (300 MHz, CDCl₃): δ 2.52 (d, J = 0.99 Hz, 3 H), 7.00–7.07 (m, 1 H). ¹³C NMR (75 MHz, CDCl₃): δ 18.43, 139.41, 172.22, 216.66. Calc. 148, found 149 [M+H]⁺.

4-(4-Nitrophenyl)-3H-1,2-dithiole-3-thione, 4a [42]

Prepared from **1a** [43]. Red solid (92 %). Mp 152–154 °C. R_f = 0.37 (20 % EtOAc/Hex). ¹H NMR (300 MHz, CDCl₃): δ 7.89 (d, J = 8.73 Hz, 2 H), 8.30 (ds, J = 8.90 Hz, 2 H), 9.34 (s, 1 H). ¹³C NMR (75 MHz, CDCl₃): δ 128.67, 135.59, 145.44, 151.15, 152.50, 166.47, 218.57. Calc. 255, found 256 [M+H]⁺.

4-Ethyl-3H-1,2-dithiole-3-thione, 4b [44]

Prepared from **1b** [45]. Yellow oil (81 %). R_f = 0.46 (20 % EtOAc/Hex). ¹H NMR (300 MHz, CDCl₃): δ 1.15 (t, J = 7.43 Hz, 3 H), 2.48–2.73 (m, 2 H), 8.86 (t, J = 0.82 Hz, 1 H). ¹³C NMR (75 MHz, CDCl₃): δ 13.03, 23.52, 150.79, 155.45, 215.12. Calc. 162, found 163 [M+H]⁺.

Ethyl 3-thioxo-3H-1,2-dithiole-4-carboxylate, 4c [46]

Prepared from diethyl 2-(ethoxymethylene)malonate, **1c**. Red solid (47 %). Mp 61–62 °C. R_f = 0.48 (20 % EtOAc/Hex). ¹H NMR (300 MHz, CDCl₃): δ 1.37 (t, J = 7.07 Hz, 3 H), 4.35 (q, J = 7.19 Hz, 2 H), 9.18 (s, 1 H). ¹³C NMR

(75 MHz, CDCl₃): δ 14.35, 62.12, 138.30, 160.81, 165.22, 211.31. Calc. 207, found 208 [M+H]⁺.

5-(4-Fluorophenyl)-3H-1,2-dithiole-3-thione, 5b [47]

Red solid (74 %). Mp 98–100 °C. R_f = 0.84 (20 % EtOAc/Hex). ¹H NMR (300 MHz, CDCl₃): δ 7.12–7.26 (m, 2 H) 7.39 (s, 1 H) 7.59–7.72 (m, 2 H). ¹³C NMR (75 MHz, CDCl₃): δ 116.97/117.26 (CF, d, J = 22 Hz), 129.19, 129.31, 136.13, 163.45/166.83 (CF, d, J = 254 Hz), 171.62, 215.66. Calc. 228, found 229 [M+H]⁺.

5-(Pyridin-4-yl)-3H-1,2-dithiole-3-thione, 5c [48]

Red solid (34 %). Mp decomposed. R_f = 0.09 (20 % EtOAc/Hex). ¹H NMR (300 MHz, CDCl₃): δ 7.50 (s, 1 H) 7.52–7.59 (m, 2 H) 8.81 (d, J = 5.93 Hz, 2 H). ¹³C NMR (75 MHz, CDCl₃): δ 121.02, 121.9, 145.67, 150.01, 175.25, 214.27. Calc. 211, found 212 [M+H]⁺.

5-(Furan-2-yl)-3H-1,2-dithiole-3-thione, 5d [49]

Red solid (63 %). Mp 97–100 °C. R_f = 0.71 (20 % EtOAc/Hex). ¹H NMR (300 MHz, CDCl₃): δ 6.61 (dd, J = 3.53, 1.72 Hz, 1 H), 6.95–7.02 (m, 1 H), 7.38 (s, 1 H), 7.64 (dd, J = 1.81, 0.54 Hz, 1 H). ¹³C NMR (75 MHz, CDCl₃): δ 113.53, 113.59, 133.27, 146.60, 146.71, 160.27, 214.50. Calc. 200, found 201 [M+H]⁺.

Ethyl 5-methyl-3-thioxo-3H-1,2-dithiole-4-carboxylate, 6b [50]

Red solid (78 %). Mp 64–66 °C. R_f = 0.84 (20 % EtOAc/Hex). ¹H NMR (300 MHz, CDCl₃): δ 1.37 (t, J = 7.16 Hz, 3 H), 2.57 (s, 3 H), 4.39 (q, J = 7.07 Hz, 2 H). ¹³C NMR (75 MHz, CDCl₃): δ 14.35, 19.11, 62.50, 140.80, 163.28, 174.05, 211.82. Calc. 220, found 221 [M+H]⁺.

4-Chloro-5-(4-methoxyphenyl)-3H-1,2-dithiole-3-thione, 6g [51]

Prepared from **3g** [52]. Yellow solid (91 %). Mp 125–127 °C. R_f = 0.63 (20 % EtOAc/Hex). ¹H NMR (300 MHz, CDCl₃): δ 3.90 (s, 3 H), 7.07 (d, J = 9.06 Hz, 2 H), 7.67 (d, J = 9.06 Hz, 2 H). ¹³C NMR (75 MHz, CDCl₃): δ 55.57, 114.78, 124.12, 130.39, 123.43, 162.45, 165.62, 206.59. Calc. 274, found 275 [M+H]⁺.

4-Chloro-5-phenyl-3H-1,2-dithiole-3-thione, 6h [51]

Prepared from **3h** [53]. Yellow solid (87 %). Mp 105–107 °C. R_f = 0.74 (2 % EtOAc/Hex). ¹H NMR (300 MHz, CDCl₃): δ 7.49–7.73 (m, 5 H). ¹³C NMR (75 MHz, CDCl₃): δ 127.07, 128.88, 129.49, 129.79, 131.91, 165.63, 206.88. Calc. 244, found 245 [M+H]⁺.

4-Chloro-5-ethyl-3H-1,2-dithiole-3-thione, 6i [54]

Prepared from **3i** [55]. Yellow solid (59 %). Mp 83–84 °C. R_f = 0.71 (20 % EtOAc/Hex). ¹H NMR (300 MHz,

CDCl_3): δ 1.40 (t, J = 7.52 Hz, 3 H), 2.98 (q, J = 7.61 Hz, 2 H). ^{13}C NMR (75 MHz, CDCl_3): δ 12.80, 27.99, 158.84, 171.46, 206.64. Calc. 196, found 197 $[\text{M}+\text{H}]^+$.

Ethyl 5-acetamido-3-thioxo-3H-1,2-dithiole-4-carboxylate, **6c** [56]

Compound **6a** (100 mg, 0.452 mmol) was refluxed in acetic anhydride (5 mL) for 30 min. The solution was then cooled, concentrated to dryness, and the crude material purified by column chromatography (hexanes/ethyl acetate, 3:1) to give **6c** as a red solid (104 mg, 88 %). Mp 156–157 °C. R_f = 0.39 (20 % EtOAc/Hex). ^1H NMR (300 MHz, CDCl_3): δ 1.43 (t, J = 7.16 Hz, 3 H), 2.40 (s, 3 H), 4.42 (q, J = 7.13 Hz, 2 H), 12.72 (br s, 1 H). ^{13}C NMR (75 MHz, CDCl_3): δ 14.15, 23.97, 62.68, 118.75, 166.36, 170.63, 174.56, 208.25. Calc. 263, found 264 $[\text{M}+\text{H}]^+$.

General procedure for the syntheses of dithiolethiones from nitriles, exemplified by 5-amino-4-(4-chlorophenyl)-3H-1,2-dithiole-3-thione, **6d**

To an ice-cooled suspension of NaH (263 mg, 6.58 mmol), carbon disulfide (220 μL , 3.62 mmol), and elemental sulfur (116 mg, 3.62 mmol) in DMF (5 mL) was added **3d** (500 mg, 3.29 mmol) in DMF (1 mL). The mixture was allowed to stir at 0 °C for 30 min, at which time saturated Na_2CO_3 (10 mL) was added. The mixture was then extracted with ethyl acetate (10 mL \times 3), washed with water (10 mL \times 3), dried (Na_2SO_4), filtered, concentrated, and purified by column chromatography (hexanes/ethyl acetate 4:1) to yield **6d** as a red solid (838 mg, 95 %). Mp 106–107 °C. R_f = 0.29 (20 % EtOAc/Hex). ^1H NMR (300 MHz, CDCl_3): δ 6.35 (br s, 2 H), 7.29 (d, J = 8.70 Hz, 2 H), 7.48 (d, J = 8.70 Hz, 1 H). ^{13}C NMR (75 MHz, CDCl_3): δ 130.00, 132.22, 132.27, 134.85, 151.04, 175.69, 234.84. Calc. 259, found 260 $[\text{M}+\text{H}]^+$.

5-Amino-4-(phenylsulfonyl)-3H-1,2-dithiole-3-thione, **6e** [30]

Red solid (69 %). Mp decomposed. R_f = 0.13 (20 % EtOAc/Hex). ^1H NMR (300 MHz, CDCl_3): δ 7.50–7.78 (m, 3 H), 7.91–8.05 (m, 2 H), 9.01 (bs 1 H), 10.09 (bs, 1 H). ^{13}C NMR (75 MHz, CDCl_3): δ 117.75, 127.39, 128.77, 133.74, 140.45, 180.23, 203.60. Calc. 289, found 290 $[\text{M}+\text{H}]^+$.

Biological methods

Cell culture conditions

The SH-SY5Y human neuroblastoma cell line was obtained from the American Type Culture Collection (ATCC, Manassas, VA). Cells were grown in DMEM:F-12 media (1:1) supplemented with FBS (10 %) and 100 U/mL penicillin and 100 $\mu\text{g}/\text{mL}$ streptomycin in 150 cm^2 culture flasks in a humidified atmosphere of 5 % CO_2 . The

media was replaced every 3–4 days, and cells were sub-cultured once a confluence of 70–80 % was reached. All test compounds were dissolved in DMSO and diluted in media (final DMSO concentration of 0.1 % v/v).

Measurement of intracellular GSH levels

SH-SY5Y cells were seeded in white 96-well plates and allowed to adhere overnight. Media was removed and replaced with media containing either test compounds (100 μM) or DMSO (0.1 %) for 24 h. Total glutathione levels (GSH + GSSG) were then measured using GSH/GSSG Glo[®] assay from Promega (Madison, WI). GSH levels were expressed as a percentage of control.

Neuroprotection assay

SH-SY5Y cells were seeded in white 96 well plates and allowed to attach overnight. Media was removed and replaced with media containing either test compounds (100 μM) or DMSO for 24 h. Next, 6-OHDA (Aldrich) in media (final concentration of 40 μM) of media was added and the cells were co-treated for 24 h. Cellular viability was assessed using the CellTiter Glo[®] assay from Promega (Madison, WI). Viability was expressed as a percentage of control.

Statistical analyses

One-way analysis of variance (ANOVA) was used to test for significant differences using GraphPad Prism software (La Jolla, CA). P values less than 0.05 were considered to be statistically significant. Results are expressed as mean \pm SEM.

Abbreviations

6-OHDA: 6-hydroxydopamine; ARE: antioxidant response element; BSO: buthionine sulfoximine; DA: dopamine; DTTs: dithiolethiones; EDGs: electron donating groups; EWGs: electron withdrawing groups; GCL: glutamate cysteine ligase; GPx: glutathione peroxidase; GSH: glutathione; GSSG: oxidized glutathione; GST: glutathione S-transferase; Keap1: Kelch-like ECH-associated protein-1; NQO1: NAD(P)H:quinone oxidoreductase; Nrf2: nuclear factor-erythroid-2 related factor-2; PD: Parkinson's disease; ROS: reactive oxygen species.

Authors' contributions

DB and HM synthesized target molecules; DB, SB, and PK performed the pharmacological characterization of molecules; DB, SB and JY provided guidance for the project; DB and JY wrote the paper. All authors read and approved the final manuscript.

Author details

¹ Department of Pharmaceutical Sciences, Manchester University College of Pharmacy, 10627 Diebold Rd, Fort Wayne, IN 46845, USA. ² Department of Microbiology and Immunology, Indiana University School of Medicine, 2101 E. Coliseum Blvd, Fort Wayne, IN 46805, USA.

Acknowledgements

The authors are grateful for Manchester University College of Pharmacy for funding this work.

Competing interests

The authors declare that they have no competing interests.

Received: 12 February 2016 Accepted: 5 October 2016

Published online: 19 October 2016

References

- Jenner P, Dexter DT, Sian J, Schapira AHV, Marsden CD (1992) Oxidative stress as a cause of nigral cell death in Parkinson's disease and incidental Lewy body disease. *Ann Neurol* 32:S82–S87
- Fahn S, Cohen G (1992) The oxidant stress hypothesis in Parkinson's disease: evidence supporting it. *Ann Neurol* 32:804–812
- Abou-Sleiman PM, Muqit MMK, Wood NW (2006) Expanding insights of mitochondrial dysfunction in Parkinson's disease. *Nat Rev Neurosci* 7:207–219
- Spillantini MG, Schmidt ML, Lee VMY, Trojanowski JQ, Jakes R, Goedert M (1997) α -Synuclein in Lewy bodies. *Nature* 388:839–840
- Hirsch EC, Vyas S, Hunot S (2012) Neuroinflammation in Parkinson's disease. *Parkinsonism Relat Disord* 18(Supplement 1):S210–S212
- Ayton S, Lei P, Adlard P, Volitakis I, Cherny R, Bush A, Finkelstein D (2014) Iron accumulation confers neurotoxicity to a vulnerable population of nigral neurons: implications for Parkinson's disease. *Mol Neurodegener* 9:27
- Fowler CJ, Wiberg Å, Orelund L, Marcusson J, Winblad B (1980) The effect of age on the activity and molecular properties of human brain monoamine oxidase. *J Neural Transm* 49:1–20
- Dexter DT, Carter CJ, Wells FR, Javoy-Agid F, Agid Y, Lees A, Jenner P, Marsden CD (1989) Basal lipid peroxidation in substantia nigra is increased in Parkinson's disease. *J Neurochem* 52:381–389
- Good PF, Hsu A, Werner P, Perl DP, Olanow CW (1998) Protein nitration in Parkinson's disease. *J Neuropathol Exp Neurol* 57:338–342
- Alam ZI, Jenner A, Daniel SE, Lees AJ, Cairns N, Marsden CD, Jenner P, Halliwell B (1997) Oxidative DNA damage in the parkinsonian brain: an apparent selective increase in 8-hydroxyguanine levels in substantia nigra. *J Neurochem* 69:1196–1203
- Chakravarthi S, Jessop CE, Bulleid NJ (2006) The role of glutathione in disulphide bond formation and endoplasmic-reticulum-generated oxidative stress. *EMBO Rep* 7:271–275
- Dagnino-Subiabre A, Cassels BK, Baez S, Johansson A-S, Mannervik B, Segura-Aguilar J (2000) Glutathione transferase m2-2 catalyzes conjugation of dopamine and dopa *o*-quinones. *Biochem Biophys Res Commun* 274:32–36
- Rotruck JT, Pope AL, Ganther HE, Swanson AB, Hafeman DG, Hoekstra WG (1973) Selenium: biochemical role as a component of glutathione peroxidase. *Science* 179:588–590
- Perry TL, Godin DV, Hansen S (1982) Parkinson's disease: a disorder due to nigral glutathione deficiency? *Neurosci Lett* 33:305–310
- Wasserman WW, Fahl WE (1997) Functional antioxidant responsive elements. *Proc Natl Acad Sci USA* 94:5361–5366
- Friling RS, Bensimon A, Tichauer Y, Daniel V (1990) Xenobiotic-inducible expression of murine glutathione *s*-transferase γ subunit gene is controlled by an electrophile-responsive element. *Proc Natl Acad Sci USA* 87:6258–6262
- McMahon M, Itoh K, Yamamoto M, Hayes JD (2003) Keap1-dependent proteasomal degradation of transcription factor Nrf2 contributes to the negative regulation of antioxidant response element-driven gene expression. *J Biol Chem* 278:21592–21600
- Zhang DD, Hannink M (2003) Distinct cysteine residues in keap1 are required for Keap1-dependent ubiquitination of nrf2 and for stabilization of Nrf2 by chemopreventive agents and oxidative stress. *Mol Cell Biol* 23:8137–8151
- Nguyen T, Sherratt PJ, Nioi P, Yang CS, Pickett CB (2005) Nrf2 controls constitutive and inducible expression of are-driven genes through a dynamic pathway involving nucleocytoplasmic shuttling by Keap1. *J Biol Chem* 280:32485–32492
- Nguyen T, Sherratt PJ, Huang H-C, Yang CS, Pickett CB (2003) Increased protein stability as a mechanism that enhances Nrf2-mediated transcriptional activation of the antioxidant response element: degradation of Nrf2 by the 26 S proteasome. *J Biol Chem* 278:4536–4541
- Wakabayashi N, Dinkova-Kostova AT, Holtzclaw WD, Kang M-I, Kobayashi A, Yamamoto M, Kensler TW, Talalay P (2004) Protection against electrophile and oxidant stress by induction of the phase 2 response: fate of cysteines of the Keap1 sensor modified by inducers. *Proc Natl Acad Sci USA* 101:2040–2045
- Itoh K, Wakabayashi N, Katoh Y, Ishii T, Igarashi K, Engel JD, Yamamoto M (1999) Keap1 represses nuclear activation of antioxidant responsive elements by Nrf2 through binding to the amino-terminal Neh2 domain. *Genes Dev* 13:76–86
- Yu Z, Shao W, Chiang Y, Foltz W, Zhang Z, Ling W, Fantus IG, Jin T (2011) Oltipraz upregulates the nuclear respiratory factor 2 α -subunit (Nrf2) antioxidant system and prevents insulin resistance and obesity induced by a high-fat diet in c57bl/6j mice. *Diabetologia* 54:922–934
- Dong J, Yan D, S-y Chen (2011) Stabilization of Nrf2 protein by D3T provides protection against ethanol-induced apoptosis in PC12 cells. *PLoS ONE* 6:e16845
- Munday R, Zhang Y, Paonessa JD, Munday CM, Wilkins AL, Babu J (2010) Synthesis, biological evaluation, and structure–activity relationships of dithiolethiones as inducers of cytoprotective phase 2 enzymes. *J Med Chem* 53:4761–4767
- Brown DA, Betharia S, Yen J-H, Tran Q, Mistry H, Smith K (2014) Synthesis and structure–activity relationships study of dithiolethiones as inducers of glutathione in the SH-SY5Y neuroblastoma cell line. *Bioorg Med Chem Lett* 24:5829–5831
- Jalewa J, Sharma MK, Hölscher C (2016) Novel incretin analogues improve autophagy and protect from mitochondrial stress induced by rotenone in SY-SY5Y cells. *J Neurochem*. doi:10.1111/jnc.13736
- Zhao Q, Yang X, Cai D, Ye L, Hou Y, Zhang L, Cheng J, Shen Y, Wang K, Bai Y (2016) Echinacoside protects against MPP⁺-induced neuronal apoptosis via ros/atr3/chop pathway regulation. *Neurosci Bull* 32:1–14
- Curphey TJ (2002) Thionation with the reagent combination of phosphorus pentasulfide and hexamethyldisiloxane. *J Org Chem* 67:6461–6473
- Guzaev AP (2011) Reactivity of 3*H*-1,2,4-dithiazole-3-thiones and 3*H*-1,2-dithiole-3-thiones as sulfurizing agents for oligonucleotide synthesis. *Tetrahedron Lett* 52:434–437
- Hansch C, Leo A, Taft RW (1991) A survey of Hammett substituent constants and resonance and field parameters. *Chem Rev* 91:165–195
- Velayutham M, Villamena FA, Navamal M, Fishbein JC, Zweier JL (2005) Glutathione-mediated formation of oxygen free radicals by the major metabolite of oltipraz. *Chem Res Toxicol* 18:970–975
- Jia Z, Zhu H, Trush M, Misra H, Li Y (2008) Generation of superoxide from reaction of 3 *H*-1,2-dithiole-3-thione with thiols: implications for dithiolethione chemoprotection. *Mol Cell Biochem* 307:185–191
- Holland R, Navamal M, Velayutham M, Zweier JL, Kensler TW, Fishbein JC (2009) Hydrogen peroxide is a second messenger in phase 2 enzyme induction by cancer chemopreventive dithiolethiones. *Chem Res Toxicol* 22:1427–1434
- Arold L, Miranda-Vizuete A, Swoboda P, Fernandes AP (2014) Protective effects of the thioredoxin and glutaredoxin systems in dopamine-induced cell death. *Free Radic Biol Med* 73:328–336
- Aureli C, Cassano T, Masci A, Francioso A, Martire S, Cocciolo A, Chichiarrelli S, Romano A, Gaetani S, Mancini P, Fontana M, d'Erme M, Mosca L (2014) 5-S-cysteinyldopamine neurotoxicity: influence on the expression of α -synuclein and erp57 in cellular and animal models of Parkinson's disease. *J Neurosci Res* 92:347–358
- Kuang X-L, Liu F, Chen H, Li Y, Liu Y, Xiao J, Shan G, Li M, Snider BJ, Qu J, Barger SW, Wu S (2014) Reductions of the components of the calreticulin/calnexin quality-control system by proteasome inhibitors and their relevance in a rodent model of Parkinson's disease. *J Neurosci Res* 92:1319–1329
- Kwon S-H, Ma S-X, Hong S-I, Kim SY, Lee S-Y, Jang C-G (2014) Eucommia ulmoides oliv. bark. attenuates 6-hydroxydopamine-induced neuronal cell death through inhibition of oxidative stress in SH-SY5Y cells. *J Ethnopharmacol* 152:173–182
- Soto-Otero R, Méndez-Álvarez E, Hermida-Ameijeiras Á, Muñoz-Patiño AM, Labandeira-García JL (2000) Autooxidation and neurotoxicity of 6-hydroxydopamine in the presence of some antioxidants. *J Neurochem* 74:1605–1612
- Drew R, Miners JO (1984) The effects of buthionine sulfoximine (BSO) on glutathione depletion and xenobiotic biotransformation. *Biochem Pharmacol* 33:2989–2994
- Nishio T (1998) Sulfur-containing heterocycles derived by reaction of ω -keto amides with Lawesson's reagent. *Helv Chim Acta* 81:1207–1214

42. Klingsberg E (1963) The 1,2-dithiolium cation. A new pseudoaromatic system. Iii. 1 conversion of dithiolium salts to quaternary pyrazolium salts and dithiolethiones. *J Org Chem* 28:529–530
43. Dudley ME, Morshed MM, Brennan CL, Islam MS, Ahmad MS, Atuu M-R, Branstetter B, Hossain MM (2004) Acid-catalyzed reactions of aromatic aldehydes with ethyl diazoacetate: an investigation on the synthesis of 3-hydroxy-2-arylacrylic acid ethyl esters. *J Org Chem* 69:7599–7608
44. Saquet M (1966) Organic sulfur compounds. Xi. Condensation of carbon disulfide with aldehydes. Synthesis of 4-aryl-1,2-dithiole-3-thiones. *Bull Soc Chim Fr* 1582–1587
45. Shimada N, Stewart C, Bow WF, Jolit A, Wong K, Zhou Z, Tius MA (2012) Neutral Nazarov-type cyclization catalyzed by palladium(0). *Angew Chem Int Ed Engl* 51:5727–5729
46. Curphey TJ (1993) Synthesis of 3*H*-1,2-dithiole-3-thiones by a novel oxidative cyclization. *Tetrahedron Lett* 34:7231–7239
47. Nuhrich A (1992) Synthesis and *in vitro* anti-hiv evaluation of disulfide linked derivatives of 1,2-dithiol-3-ylidene ketones containing a 2,3-dichloro-4-phenoxyacetic acid moiety. *Eur J Med Chem* 27:857–860
48. Legrand L (1955) Sulfuration of organic compounds. VII. 1,2-Dithiole-3-thiones with aliphatic or pyridine substituents. *Bull Soc Chim Fr* 79–83
49. Zayed SE (2014) Oxoketene dithiols: synthesis of some heterocycles as antimicrobials utilizing shrimp chitin as a natural catalyst. *Phosphorus, Sulfur Silicon Relat Elem* 189:1682–1698
50. Thuillier A (1962) Organic sulfur compounds. V. Condensation of carbon disulfide with acetone. *Bull Soc Chim Fr* 2182–2186
51. Quiniou H (1963) Heterocyclic sulfur compounds. X. The action of chlorine and bromine on several 5-aryl-1,2-dithiole-3-thiones. *Bull Soc Chim Fr* 1167–1171
52. Jiang Y, Chen X, Zheng Y, Xue Z, Shu C, Yuan W, Zhang X (2011) Highly diastereoselective and enantioselective synthesis of α -hydroxy β -amino acid derivatives: Lewis base catalyzed hydrosilylation of α -acetoxy β -enamino esters. *Angew Chem Int Ed Engl* 50:7304–7307
53. Feske BD, Kaluzna IA, Stewart JD (2005) Enantiodivergent, biocatalytic routes to both taxol side chain antipodes. *J Org Chem* 70:9654–9657
54. Trebaul C (1969) Heterocyclic sulfur compounds. Iv. Reaction of phosphorus pentasulfide with β -oxo esters containing an α -chloro, α -cyano, or an α -ethoxycarbonyl group. *Bull Soc Chim Fr* 2456–2462
55. Perrone MG, Santandrea E, Dell'Uomo N, Giannessi F, Milazzo FM, Sciarroni AF, Scilimati A, Tortorella V (2005) Synthesis and biological evaluation of new clofibrate analogues as potential PPAR α agonists. *Eur J Med Chem* 40:143–154
56. Cmelik R (2003) Syntheses and structure study on 3,3a,4,4-trithia-1-azapentalenes and their 3-oxa analogues. *Collect Czech Chem Commun* 68:1243–1263

Submit your manuscript to a SpringerOpen[®] journal and benefit from:

- Convenient online submission
- Rigorous peer review
- Immediate publication on acceptance
- Open access: articles freely available online
- High visibility within the field
- Retaining the copyright to your article

Submit your next manuscript at ► springeropen.com